JOURNAL PRE-PROOF

This is an early version of the article, published prior to copyediting, typesetting, and editorial correction. The manuscript has been accepted for publication and is now available online to ensure early dissemination, author visibility, and citation tracking prior to the formal issue publication.

It has not undergone final language verification, formatting, or technical editing by the journal's editorial team. Content is subject to change in the final Version of Record.

To differentiate this version, it is marked as "PRE-PROOF PUBLICATION" and should be cited with the provided DOI. A visible watermark on each page indicates its preliminary status.

The final version will appear in a regular issue of *Archives of Acoustics*, with final metadata, layout, and pagination.

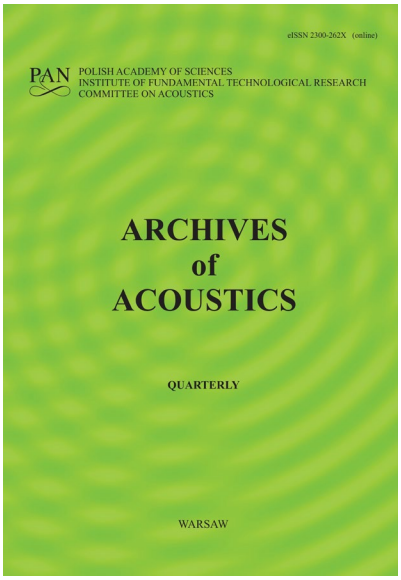

Title: A Study of Damage Modes Recognition of Polypropylene Fiber Reinforced Recycled Aggregate Concrete Based on Principal Components of Acoustic Emission Signals

Author(s): Qianxu Chen, Xin Yang

DOI: https://doi.org/10.24423/archacoust.2026.4407

Journal: *Archives of Acoustics*

ISSN: 0137-5075, e-ISSN: 2300-262X

Publication status: In press

Received: 2026-01-04

Revised: 2026-03-19

Accepted: 2026-03-20

Published pre-proof: 2026-03-25

Please cite this article as:

Chen Q., Yang X. (2026), A Study of Damage Modes Recognition of Polypropylene Fiber Reinforced Recycled Aggregate Concrete Based on Principal Components of Acoustic Emission Signals, *Archives of Acoustics*, https://doi.org/10.24423/archacoust.2026.4407

Copyright © 2026 The Author(s).
This work is licensed under the Creative Commons Attribution 4.0 International CC BY 4.0.

A study of damage modes recognition of polypropylene fiber reinforced recycled aggregate concrete based on principal components of acoustic emission signals

Qianxu Chen[1], Xin Yang[2*]

1 James Watt School of Engineering, University of Glasgow, Glasgow G12 8QQ, United Kingdom.

2 Institute of Marine and Environmental Geotechnical Engineering, Fujian University of Technology, Fuzhou 350118, China

*Corresponding author: Xin Yang, Institute of Marine and Environmental Geotechnical Engineering, Fujian University of Technology, Fuzhou 350118, China

E-mail: yangxin546@163.com

Abstract: To investigate the principal components of acoustic emission (AE) signals and damage modes of polypropylene fiber (PPF) reinforced recycled concrete, ten groups of specimens with coarse aggregate (CA) replacement rates of 0% and 25% and different particle sizes were designed and fabricated. Uniaxial compression AE tests were conducted to obtain the AE parameters during the fracture process of PPF reinforced recycled concrete. In this study, the Pearson correlation coefficient was employed to investigate the correlations among AE parameters. Then, the principal component analysis (PCA) was performed on the AE signals to conduct dimensionality reduction of the multi-dimensional data. On this basis, the optimal number of clusters for the principal components of AE signals was determined based on the silhouette coefficient. Finally, the K-means clustering algorithm was introduced to perform cluster analysis on the principal components of AE signals of PPF reinforced recycled concrete. The clustering results were compared with each

PRE-PROOF PUBLICATION

PRE-PROOF PUBLICATION ARCHIVES OF ACOUSTICS

other to explore the characteristics of each cluster and identify the corresponding damage mode for each cluster. The discriminability of AE parameters with respect to damage modes was investigated, and the research findings can provide a reference for predicting the fracture mechanism of PPF reinforced recycled concrete.

Keywords: Polypropylene fiber reinforced recycled concrete; acoustic emission; Pearson correlation coefficient; principal component analysis; K-means clustering

1. Introduction

At present, the factors restricting the widespread application of recycled concrete lie in the fact that its mechanical properties, such as compressive strength and tensile strength, are inferior to those of natural concrete. To address this problem, methods like adding external fibers can be adopted. Adding polypropylene fiber (PPF) to recycled concrete is a relatively common method (Wang et al., 2022).

In recent years, numerous scholars had investigated the characteristics of acoustic emission (AE) signals in fiber reinforced concrete, including principal component analysis (PCA) (Tayfur et al., 2018), digital image technology (Ashraf and Rucka, 2024; Sagar et al., 2025), b-value (Ashraf and Rucka, 2023), 3D printing technology (Ingle and Prem, 2025), shear model (Kantekin and Bakir, 2025), fatigue behavior (Džolan et al., 2024), three-point bending test (Umar et al., 2023), and durability (Chkhachirou et al., 2025). Zheng et al. (2022) distinguished two types of acoustic events, matrix cracking and steel fiber vibration according to AE technique. Zaki et al. (2023) utilized rise time/amplitude analysis to classify the damage modes.

PRE-PROOF PUBLICATION

PRE-PROOF PUBLICATION ARCHIVES OF ACOUSTICS

Kouta et al. (2021) found that both AE activity and fracture energy increase with the rise in fiber content and fiber length. Saha and Sagar (2021) classified the AE signals generated by fiber reinforced concrete into two categories via machine learning methods: cement matrix cracking and fiber pull-out, and pointed out that the classification of AE waveforms might facilitate the understanding of damage evolution during the fracture process.

In summary, AE parameters was obtained in this paper by conducting AE monitoring tests on PPF reinforced recycled concrete. Based on methods including the Pearson correlation coefficient, PCA, and K-means clustering, an analysis was conducted on the principal components of AE parameters and the corresponding damage modes of PPF reinforced recycled concrete, and the research findings can provide a reference for predicting the fracture mechanism of PPF reinforced recycled concrete.

2. Experimental details

2.1. Sample preparation

The PPF employed in this experiment were manufactured by Shandong Runlin Wood Industry Co., Ltd., and the main properties are presented in Table 1.

Table 1 Physical and mechanical parameters of PPFs

Fiber type	Diameter (mm)	Length (mm)	Tensile strength (MPa)	Fracture strength (MPa)	Elongation at break (%)	Initial modulus (GPa)	Density (g/cm^3)	Recommended dosage (kg/m^3)
micro-PPF	0.036	19	≥450	450	17	4.8	0.91	0.9
macro-PPF1	0.9	30	≥550	500	24	6.6	0.91	6.0

PRE-PROOF PUBLICATION
PRE-PROOF PUBLICATION ARCHIVES OF ACOUSTICS

macro-PPF2	0.9	50	≥550	500	24	6.6	0.91	6.0

In this experiment, ordinary Portland cement was used as the cementitious material, while medium sand from Zone II was adopted as the fine aggregate with a particle size range of 0.15 mm-4.75 mm, and the particle size range of the coarse aggregate (CA) was 5 mm-20 mm. The recycled CA was derived from waste C30 concrete, which was subjected to impurity removal, crushing, and subsequent sieving to obtain the recycled CA meeting the experimental requirements, as illustrated in Figure 1.

(a) Fine aggregates (b) Natural coarse aggregates

(c) Recycled coarse aggregates

Figure 1 Fine and coarse aggregates of recycled concrete

The concrete was prepared with a strength grade of C30, with a total of ten

PRE-PROOF PUBLICATION

PRE-PROOF PUBLICATION ARCHIVES OF ACOUSTICS

groups of specimens fabricated. The mix proportions were calculated as follows: 358 kg/m³ of cement, 706.15 kg/m³ of medium sand, 1120.85 kg/m³ of CA, and 215 kg/m³ of water.The water-cement ratio was kept constant at 0.6 for all groups of specimens, while the variables were the CA replacement rate and fiber content. Specifically, the replacement rates of recycled CA were set at 0 and 25%, labeled as R-0 and R-25, respectively. In this experiment, both natural CA and recycled CA had a particle size range of 5 mm-20 mm, with the proportion of the 5 mm-10 mm fraction to the 10 mm-20 mm fraction being 1:1. Specimen R-X-1 was a plain concrete specimen with no PPF added. Specimen R-X-2 incorporated micro fibers at a dosage of 0.9 kg/m^3, while Specimen R-X-3 incorporated macro fibers at a dosage of 6 kg/m^3. In addition, Specimens R-X-4 and R-X-5 incorporated a hybrid blend of macro and micro fibers, with the total fiber dosage maintained at 6 kg/m^3, and the specific mix proportions are provided in Table 2. Each group tested once for PCA.

Table 2 Mix proportions and of test specimens

Specimen No.	CA (kg/m^3)		Fiber length and fiber diameter (mm)	Fiber dosage (kg/m^3)	Compressive strength (MPa)
	Natural 5-10mm/ 10-20mm	Recycled 5-10mm/ 10-20mm			
Zero CA substitution					
R-0-1	560/560	0	None	0	37.68
R-0-2	560/560	0	19/0.036	0.9	38.99
R-0-3	560/560	0	50/0.9	6	45.94
R-0-4	560/560	0	19/0.036+30/0.9	0.9+5.1	42.92
R-0-5	560/560	0	19/0.036+50/0.9	0.9+5.1	41.13

PRE-PROOF PUBLICATION
PRE-PROOF PUBLICATION ARCHIVES OF ACOUSTICS

25% CA substitution					
R-25-1	420/420	140/140	None	0	33.23
R-25-2	420/420	140/140	19/0.036	0.9	35.56
R-25-3	420/420	140/140	50/0.9	6	44.09
R-25-4	420/420	140/140	19/0.036+30/0.9	0.9+5.1	43.46
R-25-5	420/420	140/140	19/0.036+50/0.9	0.9+5.1	51.75

2.2. Tests

In accordance with the requirements of GB/T 50081-2019 (2019), cube specimens with a side length of 150 mm were prepared. After the concrete mixture was poured into the molds, the specimens were cured at room temperature for one day. Subsequently, the specimens were demolded, labeled, and then subjected to natural curing in a curing room for 28 days. A compression testing machine HCT306B (Figure 2) was employed for the uniaxial compression test, with a loading rate of 0.5 MPa/s. An AMSY-6 AE testing system was adopted for AE monitoring, and the threshold of the AE instrument was set at 40 dB with a sampling frequency of 5 MHz to minimize the impact of ambient noise during the test.

Figure 2 HCT306B press

3. Damage mode identification based on AE parameters

PRE-PROOF PUBLICATION

PRE-PROOF PUBLICATION ARCHIVES OF ACOUSTICS

3.1. Preliminary screening of AE parameters based on the Pearson correlation coefficient method

The Pearson correlation coefficient can reflect the degree of linear correlation between two variables; its value ranges from -1 to 1, with a larger absolute value indicating a stronger correlation. Therefore, the Pearson correlation coefficient method can be adopted for the preliminary screening of AE characteristic parameters, with the aim to select parameters with low correlation coefficients and high mutual independence as far as possible, thereby reducing the size of the characteristic parameter set. Equation (1) presents the calculation formula for the Pearson correlation coefficient r. When r=1, it indicates a perfect positive linear correlation between the two variables; when r=-1, it indicates a perfect negative linear correlation; and when r=0, it indicates no linear correlation between them.

$$r = \frac{\sum_{i=1}^{n}(x_i - \bar{x})(y_i - \bar{y})}{\sqrt{\sum_{i=1}^{n}(x_i - \bar{x})^2 \sum_{i=1}^{n}(y_i - \bar{y})^2}} \tag{1}$$

Where, x_i and y_i represent the i-th observed values of the two variables x and y, respectively; $\bar{x}$ and $\bar{y}$ denote the sample means of variables x and y; and n is the sample size.

In this paper, six AE characteristic parameters, namely amplitude, rise time, duration, count, energy and dominant frequency, were selected for Pearson correlation coefficient analysis. These parameters characterize the AE signals in multiple aspects in both the time domain and frequency domain, and are thus capable of comprehensively reflecting the AE behaviors during the damage process.

Table 3 Pearson correlation coefficients between different AE parameters

Specimen	Amplitude	Rise	Duration	Count	Energy

PRE-PROOF PUBLICATION

PRE-PROOF PUBLICATION ARCHIVES OF ACOUSTICS

No.		time				
R-0-1	Rise time	0.43				
	Duration	0.75	0.63			
	Count	0.87	0.5	0.84		
	Energy	0.53	0.13	0.26	0.51	
	Dominant frequency	0.17	0.1	0.16	0.22	0.1
R-0-2	Rise time	0.63				
	Duration	0.84	0.75			
	Count	0.87	0.7	0.94		
	Energy	0.55	0.31	0.39	0.51	
	Dominant frequency	-0.05	-0.1	-0.11	-0.02	0.03
R-0-3	Rise time	0.19				
	Duration	0.57	0.36			
	Count	0.71	0.27	0.75		
	Energy	0.5	-0.01	0.13	0.37	
	Dominant frequency	0.21	0.03	0.14	0.29	0.1
R-0-4	Rise time	0.06				
	Duration	0.4	0.21			
	Count	0.49	0.08	0.58		
	Energy	0.38	-0.03	0.05	0.23	
	Dominant frequency	-0.01	-0.01	0.1	0.27	-0.03
R-0-5	Rise time	0.08				
	Duration	0.34	0.17			
	Count	0.77	0.09	0.38		
	Energy	0.32	0.02	0.05	0.15	
	Dominant frequency	0.31	0.01	0.06	0.51	0.02

PRE-PROOF PUBLICATION

PRE-PROOF PUBLICATION ARCHIVES OF ACOUSTICS

R-25-1	Rise time	0.03				
	Duration	0.17	0.09			
	Count	0.58	0.02	0.3		
	Energy	0.66	0.02	0.04	0.51	
	Dominant frequency	0.08	-0.05	0.06	0.27	0.07
R-25-2	Rise time	0.04				
	Duration	0.42	0.18			
	Count	0.49	0.07	0.6		
	Energy	0.48	-0.02	0.07	0.17	
	Dominant frequency	0.01	0.002	0.07	0.22	-0.06
R-25-3	Rise time	0.35				
	Duration	0.67	0.49			
	Count	0.75	0.41	0.83		
	Energy	0.47	0.08	0.19	0.42	
	Dominant frequency	0.005	0.01	-0.02	-0.01	0.07
R-25-4	Rise time	0.11				
	Duration	0.47	0.21			
	Count	0.48	0.11	0.64		
	Energy	0.49	0.001	0.09	0.11	
	Dominant frequency	-0.09	-0.1	0.02	0.1	-0.17
R-25-5	Rise time	0.52				
	Duration	0.78	0.69			
	Count	0.8	0.65	0.93		
	Energy	0.47	0.21	0.29	0.45	
	Dominant frequency	-0.13	-0.12	-0.18	-0.13	-0.03

PRE-PROOF PUBLICATION

PRE-PROOF PUBLICATION ARCHIVES OF ACOUSTICS

Table 3 presents the Pearson correlation coefficients among the six AE characteristic parameters, namely amplitude, rise time, duration, count, energy, and dominant frequency. Based on the values of the correlation coefficients, parameters with a coefficient greater than 0.6 were regarded as having a strong correlation, in which case one of the characteristic parameters could be discarded. As can be seen from Table 3, the Pearson correlation coefficients between the three parameters (rise time, energy, and dominant frequency) and the other parameters are mostly less than 0.6, indicating low correlation and high independence of these three parameters. The Pearson correlation coefficients among the three parameter pairs-amplitude and count, amplitude and duration, and count and duration-are mostly greater than 0.6, indicating a strong correlation between each pair. Among these parameters, amplitude and count have well-defined physical meanings: the higher their values, the stronger the acoustic emission activity. In contrast, duration generally needs to be interpreted comprehensively in combination with other parameters. Therefore, five AE characteristic parameters, namely amplitude, rise time, count, energy and dominant frequency, were selected for PCA.

3.2. Selection of characteristic parameters based on PCA

PCA is a data dimensionality reduction method that transforms standardized parameter data into several uncorrelated principal component variables via dimensionality reduction, thus capturing most of the information inherent in the original dataset. To eliminate the influence of dimensional differences among

PRE-PROOF PUBLICATION

PRE-PROOF PUBLICATION ARCHIVES OF ACOUSTICS

different characteristic parameters, the data need to be standardized prior to performing PCA.

Assuming that the original dataset is denoted as X, it is then subjected to standardization to yield the sample matrix X_{n*p}, where n is the number of samples and p is the number of features. The covariance matrix R_{p*p} is calculated according to Equation (2). The covariance matrix is subjected to eigenvalue decomposition to derive p eigenvalues, which are then sorted in descending order to obtain λ_1、$\lambda_2 \cdots \lambda_p$ and their corresponding T_1、$T_2 \cdots T_p$. At this point, the i-th calculated principal component can be expressed by Equation (3), while the contribution rate of the principal component, φ_k, can be expressed by Equation (4).

$$R_{p*p} = \frac{1}{n-1} X^T_{n*p} X_{n*p} \tag{2}$$

$$PCA(i) = T_{1i} X_1 + T_{2i} X_2 + \cdots + T_{pi} X_p \tag{3}$$

$$\varphi_k = \frac{\lambda_k}{\sum_{i=1}^{p} \lambda_i} \tag{4}$$

Where, φ_k denotes the contribution rate of the k-th principal component.

Based on the results of the Pearson correlation coefficient analysis, five characteristic parameters, namely amplitude, rise time, count, energy, and dominant frequency, were selected for PCA. Table 4 presents the contribution rates of each principal component for the specimens. As can be seen from Table 4, the cumulative contribution rate of the first three principal components exceeds 75%, indicating that the selection of these three principal components can well retain most of the information from the original dataset.

PRE-PROOF PUBLICATION

PRE-PROOF PUBLICATION ARCHIVES OF ACOUSTICS

Table 4 The contribution of each principal component and the cumulative of the first three principal components (%)

Specimen No.	1	2	3	4	5	Cumulative of 1:3
R-0-2	56.4	20.4	13.7	6.9	2.6	90.5
R-0-3	44.7	20.5	18.5	10.9	5.4	83.7
R-0-4	35.4	22.2	20.2	13.6	8.6	77.8
R-0-5	48.8	20.5	16.6	11.1	3	85.9
R-25-2	35.9	22.7	20	13.8	7.6	78.6
R-25-3	46.2	20.4	18.2	10.4	4.8	84.8
R-25-4	35.7	23.1	19.5	14.5	7.2	78.3
R-25-5	52.6	19.8	15.8	8.3	3.5	88.2

3.3. Determination of the optimal number of clusters

In the process of conducting cluster analysis, determining a reasonable number of clusters is a key step to ensure the reliability of the results. An excessively small number of clusters may result in different damage modes being incorrectly classified into the same category. Conversely, an excessively large number of clusters may lead to the over-segmentation of the same damage mode. In this paper, the silhouette coefficient is adopted to evaluate the number of clusters. The range of the number of clusters was initially set to 2-6, and the silhouette coefficient was used to evaluate the performance of each cluster number, thereby determining the optimal number of clusters ultimately.

The silhouette coefficient (SI) is an index that calculates two metrics: the average distance between a sample and other samples within its own cluster, and the average distance between the sample and samples within the nearest neighboring cluster. It

PRE-PROOF PUBLICATION
PRE-PROOF PUBLICATION ARCHIVES OF ACOUSTICS

evaluates the compactness and separation of clustering by measuring the difference between these two distances. A larger SI indicates more reasonable sample clustering and higher clustering quality. The calculation equation for the SI is given below:

$$SI = \frac{b(i) - a(i)}{\max\{a(i), b(i)\}} \tag{5}$$

Where, a(i) denotes the average distance from sample i to other samples within the same cluster, and b(i) denotes the average distance from sample i to all samples in any other cluster.

Figure 3 presents the number of clusters calculated based on the SI index. As can be seen from Figure 3, the SI index reaches its maximum value when the number of clusters is set to 4; therefore, the optimal number of clusters is determined to be 4.

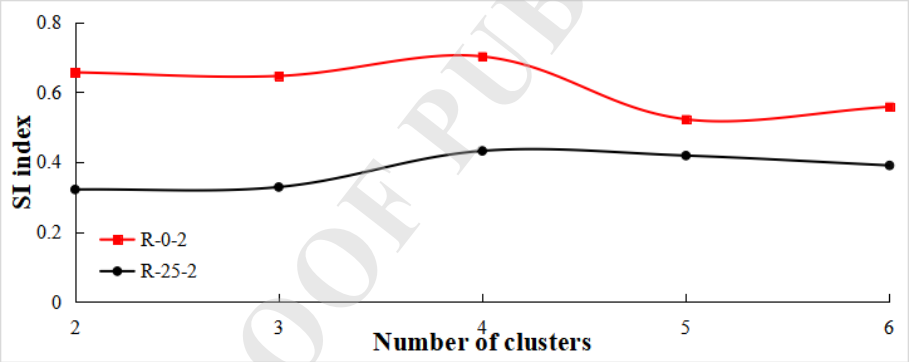

Figure 3 Number of clusters assessed by SI index

4. Analysis of clustering results

In this paper, the k-means clustering algorithm was adopted to perform cluster analysis on the results of principal component analysis of AE parameters of PPF reinforced recycled concrete, and the number of clusters was set to 4, as determined in Section 3.3.

4.1. K-means clustering

K-means is an iterative clustering algorithm whose operating principle can be outlined as follows: Given a sample dataset composed of n variables $X_1, X_2, \ldots, X_n$, the

PRE-PROOF PUBLICATION
PRE-PROOF PUBLICATION ARCHIVES OF ACOUSTICS

algorithm aims to partition these variables into k distinct clusters. Here, m_i denotes the mean value of the variables within the i-th cluster. The algorithm employs the Euclidean distance as the distance metric. The detailed steps are as follows (Wen, 2025):

(1) Initialization: Randomly and uniformly select k observation samples as the initial cluster centers m_1-m_k.

(2) Assignment: Assign each sample data point to the cluster whose center is nearest to it, based on the Euclidean distance.

(3) Update: Recalculate the mean vector (cluster center) for each cluster based on the data points assigned to it.

(4) Iteration: Repeat steps (2) and (3) until one of the following conditions is met: the predefined maximum number of iterations is reached, or the cluster centers no longer change (i.e., the mean vectors converge). Once these conditions are satisfied, the model is considered built, and the final clustering results are output.

4.2. Clustering results

Table 5 presents the characteristic ranges of the four clusters calculated by the k-means algorithm. Among these clusters, Cluster 1 is characterized by low amplitude (below 90 dB) and low energy; Cluster 2 features low dominant frequency (below 40 kHz) and high rise time; Cluster 3 is defined by high dominant frequency (above 100 kHz), relatively high amplitude (around 90 dB), and relatively high energy; Cluster 4 exhibits high amplitude (close to 100 dB) and high energy.

PRE-PROOF PUBLICATION
PRE-PROOF PUBLICATION ARCHIVES OF ACOUSTICS

Table 5 Range of clustering features

Specimen No.	AE parameters	Cluster 1	Cluster 2	Cluster 3	Cluster 4
R-0-2	Amplitude (dB)	60.1-89.6 [68.8]	69.2-100 [87.8]	70.5-100 [90.8]	99.9-100 [99.9]
	Rise time (ms)	0.01-42.5 [4.9]	0.2-104.9 [52.5]	1.1-103.8 [48.1]	0.7-104.2 [45.2]
	Count	11-5715 [4860]	1435-9182 [5629]	1685-9019 [6869]	6049-8956 [7867]
	Energy (10^6 aJ)	0.001-3.6 [0.1]	0.2-80.3 [12.8]	0.3-77.1 [20]	88.5-394 [152.4]
	Dominant frequency (kHz)	26.2-125.1 [61.5]	26.9-68.4 [35.1]	59.8-123.3 [108]	27.5-109.2 [69.9]
R-0-3	Amplitude (dB)	60.1-92.4 [77.6]	72.9-100 [88.8]	76.8-100 [89.5]	92.3-100 [99]
	Rise time (ms)	0.003-69.5 [16.5]	1.1-104.8 [63.2]	0.2-104.8 [53.8]	0.6-101.3 [42.1]
	Count	21-6523 [3324]	3476-8728 [6031]	1898-9608 [6467]	4783-9706 [7795]
	Energy (10^6 aJ)	0.008-9.7 [1.3]	0.5-46.4 [9.4]	0.8-53.9 [10.2]	13.4-467 [86.4]
	Dominant frequency (kHz)	26.2-120.2 [37.9]	28.1-72 [36.2]	62.9-123.9 [106.9]	28.1-122.7 [65.2]
R-0-4	Amplitude (dB)	60.4-100 [87.6]	81.2-100 [93.2]	79-100 [90.4]	94.5-100 [99.6]
	Rise time (ms)	0.1-101.9 [30.5]	36.3-104.8 [79.2]	0.02-104.7 [53.5]	0.1-103.2 [37.5]
	Count	64-7861 [5386]	2989-8682 [6575]	4127-8717 [6875]	5454-10023 [7946]
	Energy	0.006-32.5	1.8-171	1.1-74.8	11.6-1910

PRE-PROOF PUBLICATION

PRE-PROOF PUBLICATION ARCHIVES OF ACOUSTICS

	(10^6 aJ)	[11.9]	[26.8]	[14]	[142.3]
	Dominant	28.1-116.6	25.6-90.9	56.2-123.9	28.1-116.6
	frequency	[34.5]	[34.4]	[109.9]	[65.7]
	(kHz)				
R-0-5	Amplitude	60.2-99	71-100	69.8-100	99.1-100
	(dB)	[73.2]	[89.9]	[91.4]	[100]
	Rise time	0.01-52	0.008-104.4	1.3-104	1.9-103.4
	(ms)	[12.4]	[52.2]	[52.1]	[47.8]
	Count	92-5249	1643-9068	1256-8968	6109-8949
		[1371]	[5991]	[6803]	[7801]
	Energy	0.004-18.7	0.2-236	0.2-377	133-2600
	(10^6 aJ)	[0.5]	[30.2]	[38.5]	[522]
	Dominant	28.7-166	28.7-76.9	62.3-128.5	28.7-110.5
	frequency	[56.1]	[35]	[106.7]	[52.6]
	(kHz)				
R-25-2	Amplitude	60.4-99.2	85.1-100	77.3-100	86.7-100
	(dB)	[85.2]	[95.4]	[91.1]	[96.7]
	Rise time	0.03-104.3	49.1-104.6	0.2-104.8	0.1-84.9
	(ms)	[48.4]	[79.4]	[50.3]	[25.9]
	Count	84-7954	4128-8587	4775-8733	4294-8714
		[5562]	[6901]	[6942]	[6912]
	Energy	0.005-43.6	2.2-218	1.4-113	4.5-1030
	(10^6 aJ)	[6.2]	[43.2]	[15.9]	[66.4]
	Dominant	26.2-113.5	26.2-115.4	59.2-161.1	26.9-114.7
	frequency	[35.1]	[38.1]	[110.3]	[37.1]
	(kHz)				
R-25-3	Amplitude	60.1-94.7	75.8-100	70.6-100	95.1-100
	(dB)	[74.2]	[89.4]	[88.3]	[99.7]
	Rise time	0.01-51.5	0.1-104.8	0.3-104.4	3.5-97.8
	(ms)	[10.5]	[52.1]	[54.3]	[42.6]
	Count	26-6190	1927-9135	2429-9091	4474-9940

PRE-PROOF PUBLICATION

PRE-PROOF PUBLICATION ARCHIVES OF ACOUSTICS

		[1718]	[6282]	[5954]	[8403]
	Energy	0.002-7	0.5-109	0.3-78.4	55.1-607
	(10^6 aJ)	[0.6]	[16.4]	[10.8]	[127.3]
	Dominant	27.5-121.5	26.9-68.4	69.6-125.1	28.1-128.1
	frequency	[69.4]	[34.2]	[109.7]	[87.6]
	(kHz)				
R-25-4	Amplitude	62.1-97	80.5-100	80.3-100	91.4-100
	(dB)	[84.9]	[94.3]	[92.7]	[98.3]
	Rise time	0.05-87.7	36.1-104.8	0.3-104.2	0.3-100.6
	(ms)	[27.5]	[77.1]	[50.6]	[32.1]
	Count	74-7802	4426-8673	4952-8794	4362-8842
		[5170]	[6617]	[6964]	[6988]
	Energy	0.008-66.2	1.4-186	1.5-116	6.4-727
	(10^6 aJ)	[5.9]	[30.1]	[16.3]	[107.2]
	Dominant	28.1-125.7	28.3-109.3	37.2-192.3	28.1-122.7
	frequency	[47]	[37.3]	[111.5]	[38.5]
	(kHz)				
R-25-5	Amplitude	60-94.9	73.7-100	73.1-100	96.8-100
	(dB)	[72.7]	[88.2]	[89.1]	[99.9]
	Rise time	0.01-43.5	0.6-104.1	0.7-104.2	0.6-104.3
	(ms)	[8.4]	[49.8]	[51.6]	[47.6]
	Count	28-5326	1349-9215	1952-9253	6074-9522
		[1050]	[5806]	[6322]	[8373]
	Energy	0.002-9.5	0.3-217	0.3-192	163-968
	(10^6 aJ)	[0.5]	[14.9]	[15.9]	[389]
	Dominant	29.9-123.9	28.1-60.4	75.1-123.2	28.1-115.4
	frequency	[81.6]	[33.1]	[107.1]	[66.5]
	(kHz)				

Note: The average value is in square brackets

4.3. Damage mode identification

PRE-PROOF PUBLICATION
PRE-PROOF PUBLICATION ARCHIVES OF ACOUSTICS

Bian et al. (2021) classified the damage modes of fiber concrete into three categories: matrix cracking, fiber-matrix debonding, and fiber pull-out. Based on the findings presented in Section 4.2, Cluster 1 is characterized by low amplitude (below 90 dB) and low energy, corresponding to matrix cracking failure. Cluster 3 is characterized by high dominant frequency (above 100 kHz), relatively high amplitude (around 90 dB), and relatively high energy, corresponding to fiber-matrix debonding failure. Cluster 4 is characterized by high amplitude (close to 100 dB) and high energy, corresponding to fiber pull-out failure. Cluster 2, by contrast, is characterized by low dominant frequency (below 40 kHz) and high rise time, corresponding to mechanical noise.

As can be seen from Table 5, the AE characteristic parameters exhibit different performance levels. Both amplitude and energy can be used to distinguish the three different damage modes, namely matrix cracking, fiber-matrix debonding, and fiber pull-out; relatively speaking, however, energy demonstrates a better discrimination performance. Taking Specimen R-0-2 as an example, the average amplitude of fiber-matrix debonding is 1.32 times that of matrix cracking, and the average amplitude of fiber pull-out is 1.1 times that of fiber-matrix debonding; the average energy of fiber-matrix debonding is 200 times that of matrix cracking, and the average energy of fiber pull-out is 7.6 times that of fiber-matrix debonding. The dominant frequency can be used to distinguish mechanical noise. The average dominant frequency of mechanical noise is below 40 dB, with most values of this cluster falling

PRE-PROOF PUBLICATION

PRE-PROOF PUBLICATION ARCHIVES OF ACOUSTICS

within the range of 28-80 dB and few high-frequency events (above 100 dB). The count exhibits poor discrimination performance; matrix cracking failure is associated with a low count, while it is difficult to distinguish among the other three damage types using this parameter.

There is a certain correlation between compressive strength and matrix cracking. The lower the energy of matrix cracking, the higher the compressive strength of the specimen. Overall, the energy of R-X-3 and R-X-5 specimens is relatively low, while their compressive strength is relatively high.

5. Conclusions

This paper conducts a study on the PCA of AE parameters and damage modes of PPF reinforced recycled concrete, and draws the following conclusions:

(1) The study shows that the Pearson correlation coefficients between the three parameters (rise time, energy, and dominant frequency) and the other parameters are mostly less than 0.6, indicating low correlation and high independence of these three parameters. The Pearson correlation coefficients among the three parameter pairs-amplitude and count, amplitude and duration, and count and duration-are mostly greater than 0.6, indicating a strong correlation between each pair. Five AE characteristic parameters, namely amplitude, rise time, count, energy and dominant frequency, were selected for the PCA of PPF reinforced recycled concrete.

(2) Based on the SI index, the optimal number of clusters for the principal

PRE-PROOF PUBLICATION
PRE-PROOF PUBLICATION ARCHIVES OF ACOUSTICS

components of PPF reinforced recycled concrete was determined to be 4. The unsupervised learning algorithm of k-means clustering was applied to identify the damage modes of PPF reinforced recycled concrete, with four distinct damage modes being identified as follows: ① mechanical noise, featuring low dominant frequency (below 40 kHz) and high rise time; ② matrix cracking, characterized by low amplitude (below 90 dB) and low energy; ③ fiber-matrix debonding, exhibiting high dominant frequency (above 100 kHz), relatively high amplitude (around 90 dB) and relatively high energy; ④ fiber pull-out, with high amplitude (close to 100 dB) and high energy.

(3) The AE characteristic parameters exhibit varying discrimination performance. Both amplitude and energy can be used to distinguish the three distinct damage modes, namely matrix cracking, fiber-matrix debonding, and fiber pull-out; however, energy demonstrates a superior discrimination performance. The dominant frequency can be used to distinguish mechanical noise, whereas the count exhibits poor discrimination performance.

It should be pointed out that some conclusions of this paper need to be further verified by fiber pull-out tests.

Acknowledgements

This study was supported by the Fujian Natural Science Foundation (Grant No. 2022J01930) , the authors gratefully acknowledge this support.

PRE-PROOF PUBLICATION
PRE-PROOF PUBLICATION ARCHIVES OF ACOUSTICS

References

Ashraf S., Rucka M. (2023), Microcrack monitoring and fracture evolution of polyolefin and steel fibre concrete beams using integrated acoustic emission and digital image correlation techniques, Construction and Building Materials, **395**: 132306.

Ashraf S., Rucka M. (2024), Comparative study on fracture evolution in steel fibre and bar reinforced concrete beams using acoustic emission and digital image correlation techniques, Case Studies in Construction Materials, **20**: e03359.

Bian C., Wang J.Y., Guo J.Y. (2021), Damage mechanism of ultra-high performance fibre reinforced concrete at different stages of direct tensile test based on acoustic emission analysis, Construction and Building Materials, **267**: 120927.

Chkhachirou M., El-Hassan H., El-Maaddawy T. (2025), Durability of BFRP bars embedded in geopolymer concrete under hygrothermal exposure and sustained loading, Case Studies in Construction Materials, **23**: e05571.

Džolan A., Fischer O., Niedermeier R. (2024), Analyses of the fatigue behavior of carbon short-fiber-reinforced concrete (CSFRC) under tension and flexion, Construction and Building Materials, **453**: 139058.

GB/T 50081-2019 (2019), Code for test methods of physical and mechanical properties of concrete. Beijing, China Architecture & Building Press, 2019. (in Chinese)

PRE-PROOF PUBLICATION

PRE-PROOF PUBLICATION ARCHIVES OF ACOUSTICS

Ingle V.V., Prem P.R. (2025), Acoustic emission examination of 3D printed ultra-high performance concrete with and without coarse aggregate under fresh and hardened states, Journal of Building Engineering, **111**:113491.

Kantekin Y., Bakir B.B. (2025), Joint shear model for fiber reinforced concrete beam-column connections, Journal of Building Engineering, **101**: 111833.

Kouta N., Saliba J., Saiyouri N. (2021), Fracture behavior of flax fibers reinforced earth concrete, Engineering Fracture Mechanics, **241**: 107378.

Sagar R.V., Samadhan S.A., Kundu T. (2025), Tensile stress-crack width relationship for steel fiber reinforced concrete under mode I fracture, Mechanics Research Communications, **144**: 104378.

Saha I., Sagar R.V. (2021), Classification of the acoustic emissions generated during the tensile fracture process in steel fibre reinforced concrete using a waveform-based clustering method, Construction and Building Materials, **294**: 123541.

Tayfur S., Alver N., Adbi S., Saatci S., Ghiami A. (2018), Characterization of concrete matrix/steel fiber de-bonding in an SFRC beam: Principal component analysis and k-mean algorithm for clustering AE data, Engineering Fracture Mechanics, **194**: 73-85.

Umar H.A., Zeng X.H., Long G.C., Tang Z., Lan X.L., Zhu H.S. (2023), Synergistic effects of asphalt emulsion and fiber reinforcement on fracture properties and energy absorption of self-compacting concrete, Theoretical and Applied Fracture

PRE-PROOF PUBLICATION

PRE-PROOF PUBLICATION ARCHIVES OF ACOUSTICS

Mechanics, **127**: 104043.

Wang C.Q., Zhang Y.Y., Ma Z.M., Wang D.J. (2022), Hysteretic deteriorating behaviors of fiber-reinforced recycled aggregate concrete composites subjected to cyclic compressive loadings, Journal of Building Engineering, **49**: 104087.

Wen Y.J. (2025), Research on damage pattern identification and evolution mechanism of steel-concrete structures based on acoustic emission and machine learning, Master Thesis, Guangxi University. (in Chinese)

Zaki Y.A., Abouhussien A.A., Hassan A.A.A., Ismail M.K., AbdelAleem B.H. (2023), Crack detection and classification of repaired concrete beams by acoustic emission monitoring, Ultrasonics, **134**(5): 107068.

Zheng Q.M., Li C., He B., Jiang Z.W. (2022), Revealing the effect of silica fume on the flexural behavior of ultra-high-performance fiber-reinforced concrete by acoustic emission technique, Cement and Concrete Composites, **131**(6): 104563.

PRE-PROOF PUBLICATION

PRE-PROOF PUBLICATION ARCHIVES OF ACOUSTICS